

The Mechanics and Dynamics of Tendrils Perversion in Climbing Plants

Alain Goriely*[†] and Michael Tabor*

**University of Arizona, Program in Applied Mathematics,
Building #89, Tucson, AZ85721,*

[†]*Université Libre de Bruxelles, Département de Mathématique,
CP218/1, 1050 Brussels, Belgium*

e-mail: agoriel@ulb.ac.be, Fax:520.621.8322

Abstract

The mechanics and dynamics of the helix hand reversal (perversion) exhibited by the tendrils of climbing plants is investigated. The tendrils are modeled as thin elastic rods with intrinsic curvature and a linear and nonlinear stability analysis is performed. This system provides an example of curvature driven morphogenesis

1. Introduction

Among the many different mechanisms climbing plants use to climb and grow along supports, the so-called “tendrils-bearers” or “clingers” constitute an important class. Tendrils are tender, soft, curly and flexible organs that exhibit circumnutation in their attempt to find a support. When a tendril touches a support, such as a trellis, its tissues develop in such a way that it starts to curl and tighten up; eventually becoming robust and tough. This curling provides the plant with an elastic springlike connection to the support that enables it to resist high winds and loads (See Figure 1.) Since neither the stem nor the support can rotate, the total twist in the tendril cannot change. Therefore, as the tendril curls on itself, the coils of the spiral are reversed at some point so that the tendril goes from a left-handed helix to a right-handed, the two being separated by a small segment (See Figure 2.).

The phenomenon of helix hand reversal illustrated in the growth of tendrils was first called *perversion* by the 19th century topologist Listing; presumably after the usage of the word *perversus* to describe inverted seashell specimens in conchology. Its occurrence in climbing plants gives us a beautiful mechanical system with which to study the problem of how curvature rather than twist (such as in the formation of bacterial macrofibers or DNA [1]) can drive morphogenesis in natural systems. Indeed, we show that the main mechanical quantity driving the process is the *intrinsic curvature* of the filament (the inverse radius of the best fitting circle to a small piece of filament in its lowest relaxed energy state).

Tendrils perversion was a fascinating topic for Charles Darwin as he described it at length in his book *The Movements and Habits of Climbing Plants* [2] which was based on an essay presented at the Linnean Society in 1865. shortly after, the subject attracted the interest of eminent 19th century biologists such as Asa Gray, Hugo de Vries and Sachs. Interestingly enough, Darwin himself appears to have been unaware of the earlier history of the topic: in particular it was studied by Leon in 1858, Dutrochet in 1844, von Mohl and de Candolle in 1827. De Candolle himself attributes the first observation of the phenomenon to Ampère in

the late 18th century. Furthermore, a careful examination of the tendrils drawings of Linné in *Philosophia Botannica* (1751) (see Fig. 4) clearly shows a spiral inversion and seems to indicate that Linné was well aware of the phenomenon [5].

The equivalent of tendril perversion is nowadays recognized to occur in problems ranging from the False-twist technique in the textile industry [3] to the microscopic properties of vegetal fibers such as cotton [4]. Perhaps the most familiar occurrence of spiral inversion can be found in telephone cords. As a coiled telephone cord is first extended and untwisted and then slowly released, a spiral inversion will naturally appear: usually producing annoying snarls (see Fig. 3).

Here, we give a qualitative and quantitative description of the tendril perversion problem. The theory of thin elastic rods of Kirchhoff provides a natural framework to analyze the dynamics of the phenomenon. Indeed, we show that tendril perversion (and more generally the phenomenon of spiral inversions) can be explained in terms of a dynamical analysis of the solutions to the Kirchhoff equations for thin elastic rods. This talk is structured as follows: first the Kirchhoff model is briefly introduced, then a newly developed perturbation scheme is used to study the stability of a straight filament with intrinsic curvature under tension. Then the linear and nonlinear analysis of the tendril is performed and compare with the energetics of helices.

2. The Kirchhoff model

The Kirchhoff model of rod dynamics describes inextensible rods whose length is much greater than the cross sectional radius. Using these fundamental assumptions, all the physical quantities associated with the filament are averaged over the cross sections and attached to the central axis $x = x(s, t)$. The total force $F = F(s, t)$ and moment $M = M(s, t)$ can then be expressed in term of the local basis (see Fig 5.) The conservation of linear and angular momentum leads to the Kirchhoff equations which, in scaled variables and for a rod of circular cross-section, are [6, 7]:

$$\begin{aligned} F'' &= \ddot{d}_3, \\ M &= (\kappa_1 - \kappa_1^{(u)})d_1 + (\kappa_2 - \kappa_2^{(u)})d_2 + \Gamma(\kappa_3 - \kappa_3^{(u)})d_3, \\ M' + d_3 \times F &= d_1 \times \dot{d}_1 + d_2 \times \dot{d}_2, \end{aligned} \tag{1}$$

where $(d_1, d_2, d_3) = (N, B, T)$: respectively, the normal, binormal and tangent vector to x . κ and ω are the twist and spin vectors:

$$d_i' = \kappa \times d_i, \quad \dot{d}_i = \omega \times d_i \quad i = 1, 2, 3. \tag{2}$$

The parameter Γ measures the ratio between bending and twisting coefficients of the rod. The intrinsic curvature vector $\kappa^{(u)}$ corresponds to the configuration with the lowest elastic energy $\mathcal{E} = \int_0^L M \cdot (\kappa - \kappa^{(u)}) ds$. Here we consider the effect of a constant intrinsic curvature $(\kappa^{(u)} = (0, K, 0))$.

3. The Stability Analysis

In order to understand and analyze spiral inversion, we start with a simple stationary solution: a straight filament under tension $f_3 = \phi$ with intrinsic curvature K but no twist, *i.e.* $\gamma = 0$. As the tension is slowly released, experience shows that there is a critical tension for which the straight filament solution loses its stability and bifurcates into new solutions. In order to capture this bifurcation and analyze its dynamics we use recently developed methods to study the linear and nonlinear stability of stationary solution [8, 9, 10].

The basic idea consists of expanding the local basis $d = d^{(0)} + \epsilon d^{(1)} + \epsilon^2 d^{(2)} + \dots$ in a small parameter ϵ and requiring that to each order in ϵ , the basis $d = d(s, t)$ is orthonormal. Doing so, a linear system describing the orientation of the basis α and the perturbed forces $f^{(1)}$ can be obtained :

$$\mathcal{L}(\mu^{(0)}) \cdot \mu^{(1)} = 0, \quad (3)$$

where $\mu^{(0)} = (f^{(0)}, \kappa^{(0)})$ is the stationary solution and $\mu^{(1)} = (f^{(1)}, \alpha)$; \mathcal{L} is a linear, second-order differential operator in s and t whose coefficients depend on s through the unperturbed solution $\mu^{(0)}$.

We consider here the stationary solution: $\mu^{(0)} = (0, 0, \phi^2, 0, 0, 0)$. The solutions (to 3) can be expressed as sum of the fundamental solutions $\mu_j^{(1)} = Ax_j e^{ins + \sigma t} + c.c$ ($i = 1, \dots, 6$) where the growth rate σ is a solution of the dispersion relations, $\Delta(\sigma, n) = 0$, obtained by substituting this solution into (3). The critical value of the parameters where solutions appear are obtained by solving $\Delta(0, n) = 0$:

$$(K^2 - \Gamma n^2) = \phi \Gamma \quad (4)$$

This relationship provides valuable insight into the stability of the straight filament: If the filament is infinite, then for a fixed intrinsic curvature there exists a critical value of the $\phi_0 = \frac{K^2}{\Gamma}$, such that for all $\phi > \phi_0$, the rod is stable. For $\phi < \phi_0$ the rod becomes linearly unstable. However, if the filament is finite of length $2\pi L$, then the first unstable mode is $n = 1/L$, and the corresponding critical tension is

$$\phi_1 = \frac{L^2 K^2 - \Gamma}{L^2 \Gamma}. \quad (5)$$

As the tension is further decreased, new modes become unstable for the values $\phi_k = \frac{L^2 K^2 - k^2 \Gamma}{L^2 \Gamma}$ the last of which corresponds to $\phi = 0$, that is the largest integer less or equal to $KL/\sqrt{\Gamma}$. The solution corresponding to the first mode can be easily obtained to second-order (See Fig 6.):

$$x(s, t) = \left(s - X_n^2 \frac{\sin(2ns) + 2ns}{2n}, -2KX_n^2 \frac{\phi^2 \Gamma^2 - K^2(1 - \Gamma) \cos^2(ns)}{3\phi^4 \Gamma^2 - 7K^2 \Gamma \phi^2 + 4K^4}, -2X_n \frac{\sin(ns)}{n} \right) \quad (6)$$

where $X_n = \Re(A_n)$ and the amplitude A can be obtained by a nonlinear analysis [9]:

$$A_n^2 = \frac{4\Gamma^{3/2}(\phi - \phi_n)(K^2 + 3\Gamma n^2)(K^2 - \Gamma n^2)^{1/2}}{(12 - 7\Gamma)K^4 + 2n^2\Gamma^2(1 - 2\Gamma)K^2 - 3n^4\Gamma^3}.$$

4. Energetics of Helices

So far, we have discussed the bifurcation of a straight filament to describe the onset of instabilities. In order to give a full description of the problem, it is important to describe the two asymptotic helices. These solutions can be by analyzing a family of helicoidal solution for every given value of the tension:

$$\kappa = (0, \kappa_F, \tau_F) \quad f = \left(0, f_0, \frac{\tau_F}{\kappa_F} f_0 \right), \quad (7)$$

where $f_0 = -\tau_F(\kappa_F - K) + \Gamma\kappa_F\tau_F$. The tension $\phi = f_3$ sets the torsion: $\tau_F^2 = \frac{\phi\kappa_F}{K\Gamma}$. The corresponding elastic energy is $\mathcal{E} = 2\pi L [(\kappa_F - K)^2 + \Gamma\tau_F^2]$. The lowest energy states correspond to the helices with (κ_F, τ_F) such that: $2(\Gamma - 1)\kappa_F^3 - 2K(\Gamma - 2)\kappa_F^2 - 2\kappa_F K^2 + \Gamma\tau_F^2 K =$

0. In the (κ_F, τ_F) plane, this family of *optimal solutions* forms a closed curve passing through the points $(0, 0)$ (straight line) and $(K, 0)$ (rings). The energetics of the helices strongly suggest that the perverted tendril will in fact connect asymptotically two optimal helices (a right-handed one ($\tau_F > 0$) to a left-handed one ($\tau_F < 0$)). Moreover, for a given tension ϕ , the amount of twist contained in a half filament can be computed. The total twist Tw is given by the number of helical repeat per unit length (holding the ends, the total twist is the twist obtained by pulling the helix to a straight filament, converting helical torsion to twist density):

$$Tw^2 = \frac{L^2}{4} \left(\kappa_F^2 + \frac{\phi^2 \kappa_F}{K + \kappa_F(\Gamma - 1)} \right) \quad (8)$$

where κ_F is the curvature of the optimal solution with given tension ϕ^2 . This in turn gives the number of helical loops in half a filament: $N = \pi L Tw - 1$.

5. The perverted tendril

The two different approaches outlined above (energetics and stability analysis) can now be coupled to give a complete picture of the mechanics and dynamics of tendril perversion. For a given curvature as the tension decreases (or equivalently for given tension and increasing curvature), the straight tendril reach a critical state where it loses stability. After the onset, the shape is well described by the solutions given above. As the tension is further decreases, the central piece can still be described by the same nonlinear solutions whereas the long range solutions (the asymptotic states) are described by the helical solutions obtained by energetics consideration (See Fig. 8).

6. Conclusions

For centuries, scientists have been bewildered by the mechanical ingenuity of natural phenomena. The perversion of tendrils in climbing plants is a beautiful answer to a simple elementary mechanical question, namely: How to create a twistless spring? We showed here that the twistless spring can be simply created by a change in intrinsic curvature. The structure that results from this curvature change is a coupling of two (or more) helical springs with opposite handedness. The modeling of this phenomenon through Kirchhoff's theory of thin rods provides quantitative results on the critical parameters involved in the process as well as a complete qualitative picture of the mechanism involved. It also highlights a new scenario for morphogenesis where local curvature, rather than twist, determines the final structure. This is due to the existence of a global topological invariant (the total twist) conserved in the symmetry breaking bifurcation.

Acknowledgments: This work is supported by DOE grant DE-FG03-93-ER25174, NATO-CRG grant 97/037 and the Flinn Foundation.

References

- [1] N. H. Mendelson, Proc. Natl. Acad. Sci. USA, **75**, 2472–2482 (1978)
- [2] C. Darwin, *The movements and habits of climbing plants* New York (1888).
- [3] *Bulk, stretch and texture*, Papers of the 51st Annual conference of the Textile Institute (1966).
- [4] L. Waterkeyn, in *Cotton fibres: their development and properties* 17–22,(International Intsitute for Cotton, 1985).
- [5] A. Goriely and M. Tabor, “A brief history of perversion and handedness” (in preparation).
- [6] E. H. Dill, Arch. Hist. Exact. Sci. **44**, 2 (1992).
- [7] B. D. Coleman *et al.*, Arch. Rational Mech. Anal. **121**, 339 (1993).
- [8] A. Goriely and M. Tabor, Phys. Rev. Lett., **77**, 3537–3540 (1996). A. Goriely and M. Tabor, Physica D **105**, 20–44 (1997). A. Goriely and M. Tabor, Physica D **105**, 45–61 (1997).
- [9] A. Goriely and M. Tabor, “Nonlinear dynamics of filaments III: Instabilities of helical rods”. Proc. Roy. Soc. London (A) To be published (1998).
- [10] A. Goriely and M. Tabor, “Nonlinear dynamics of filaments IV: Spontaneous looping of twisted rods”. Proc. Roy. Soc. London (A) To be published (1998).

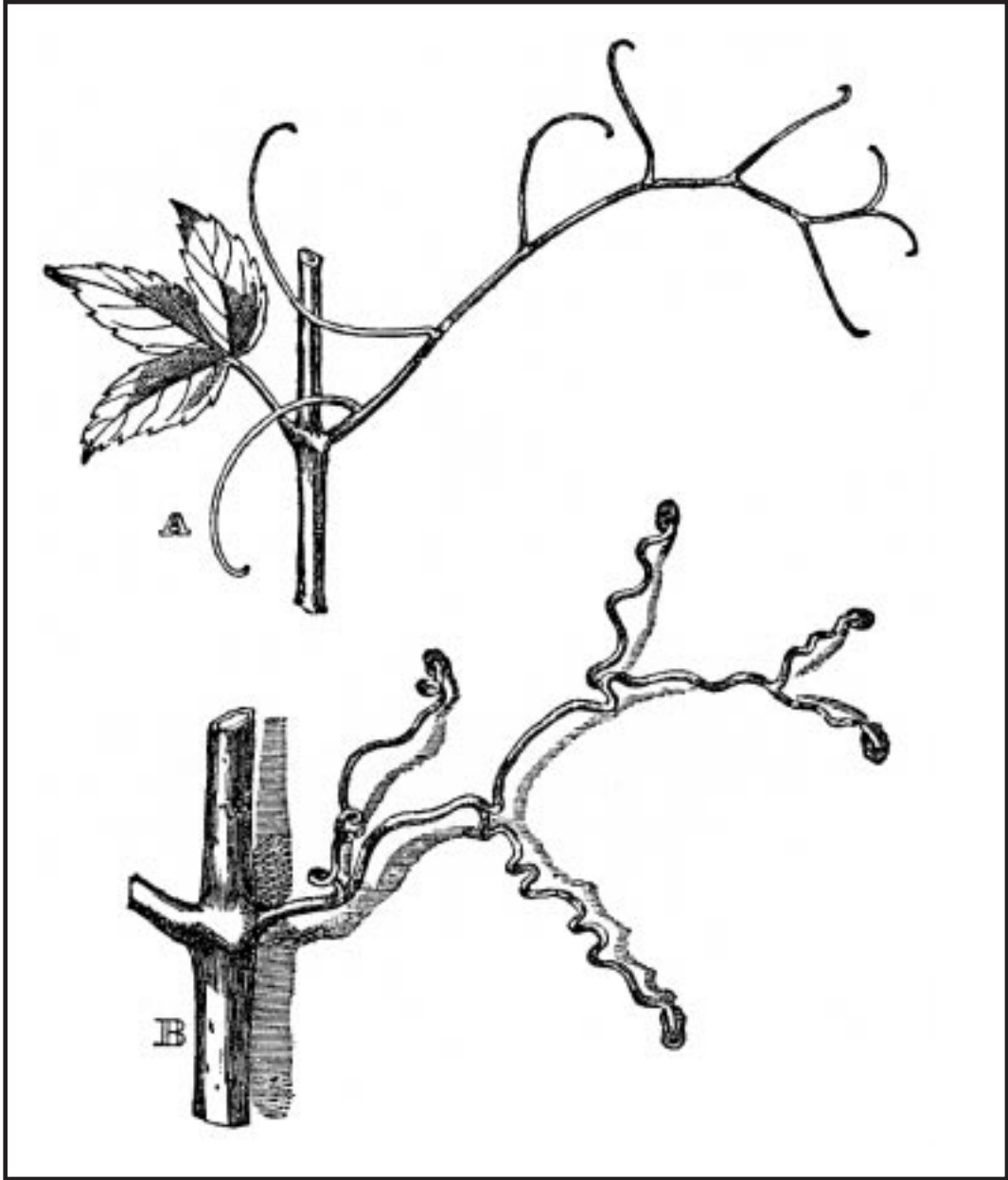


Figure 1: Tendrils in *Ampelopsis hederacea*: Young (A.) and older (B.) after their attachment to a wall. The unattached tendrils have withered and dropped off. Illustration by George Darwin in Darwin's *Habits of Climbing Plants* (1888)

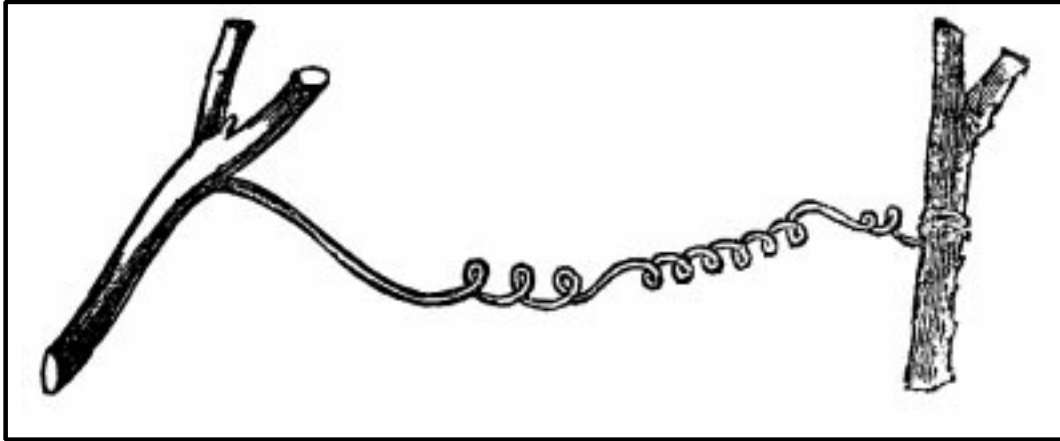


Figure 2: Tendril perversion in *Bryonia dioica* in Darwin's *Habits of Climbing Plants* (1888)



Figure 3: Perversion in a telephone cord (1998)

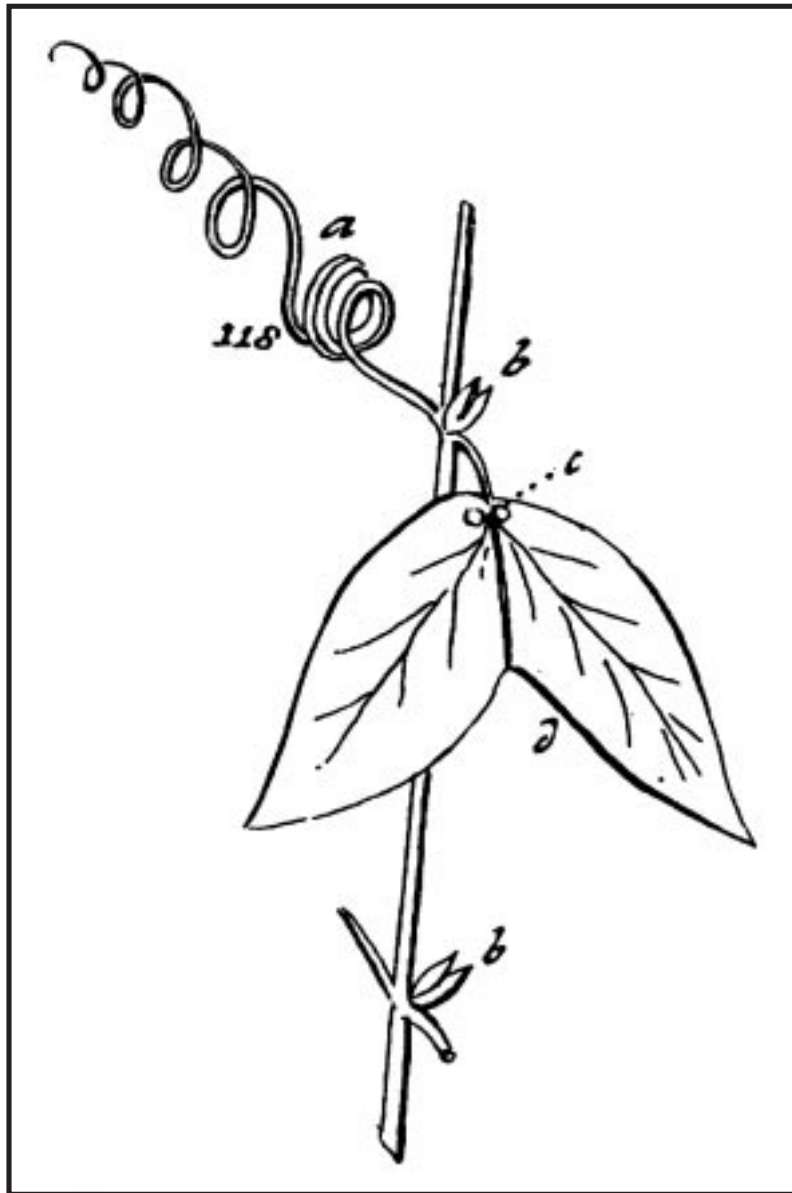
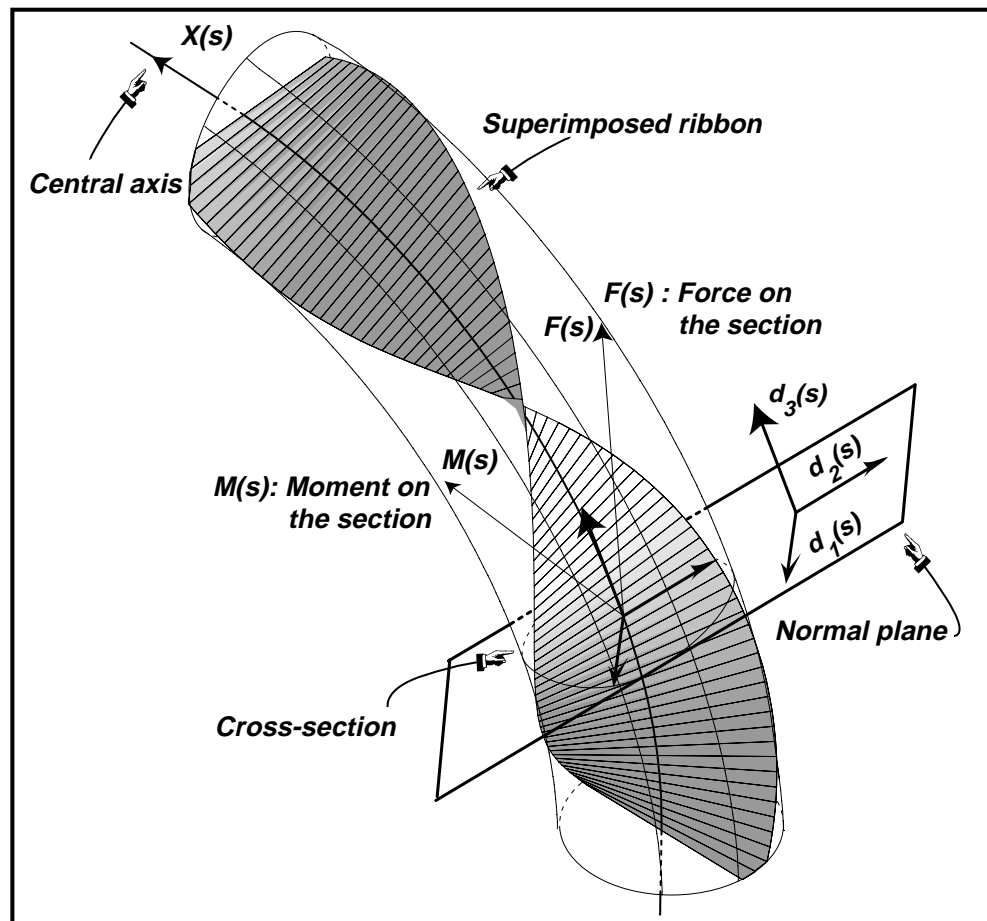


Figure 4: Tabula V. in Linné's *Philosophia Botanica* (1751)



[hb]

Figure 5: The local director basis and the force on a cross section (1751)

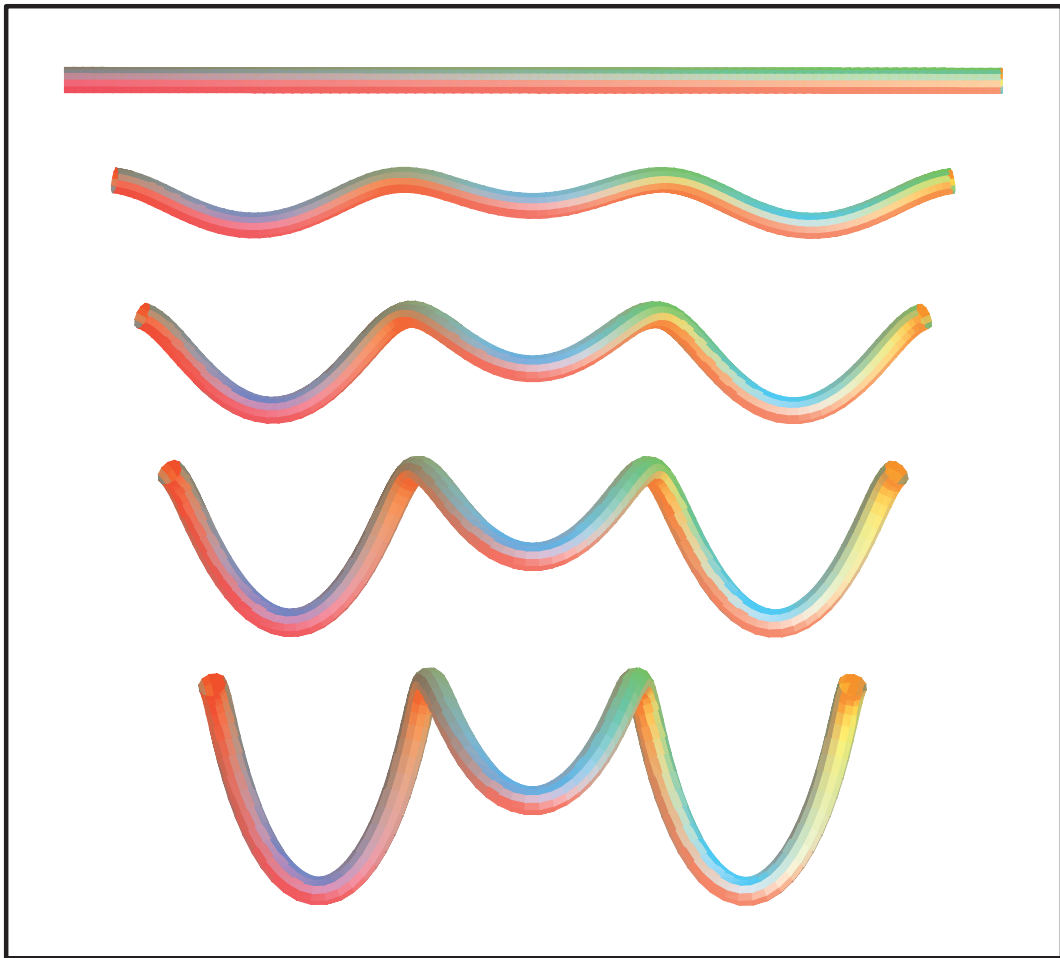


Figure 6: The second order solution for $\Gamma = 3/4$, $n = 1/8$, $\phi = 3/10$, $K = 1/4$

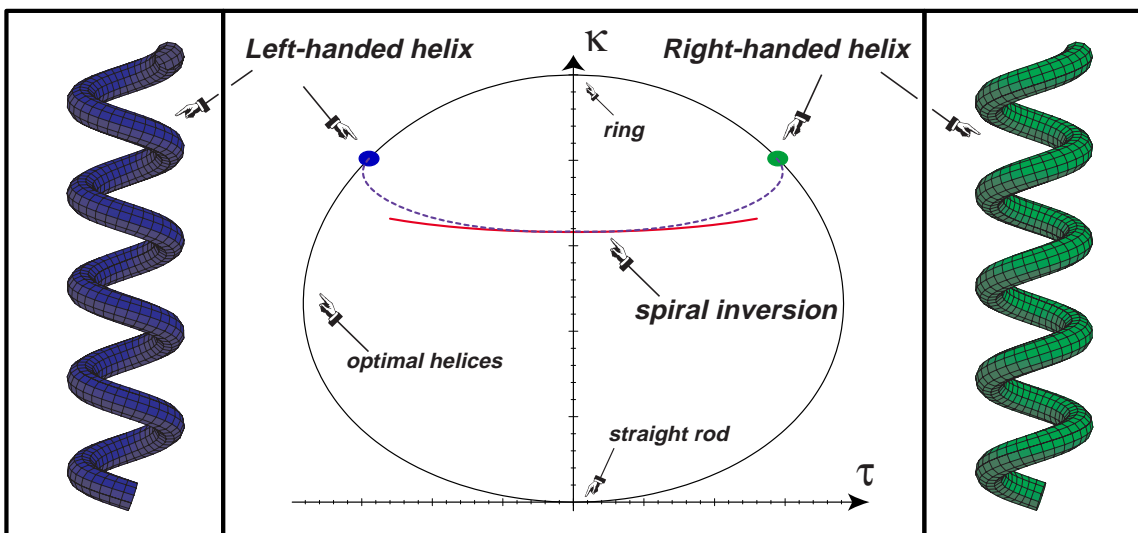


Figure 7: The two fixed points together in the curvature-torsion plane together with the optimal curve

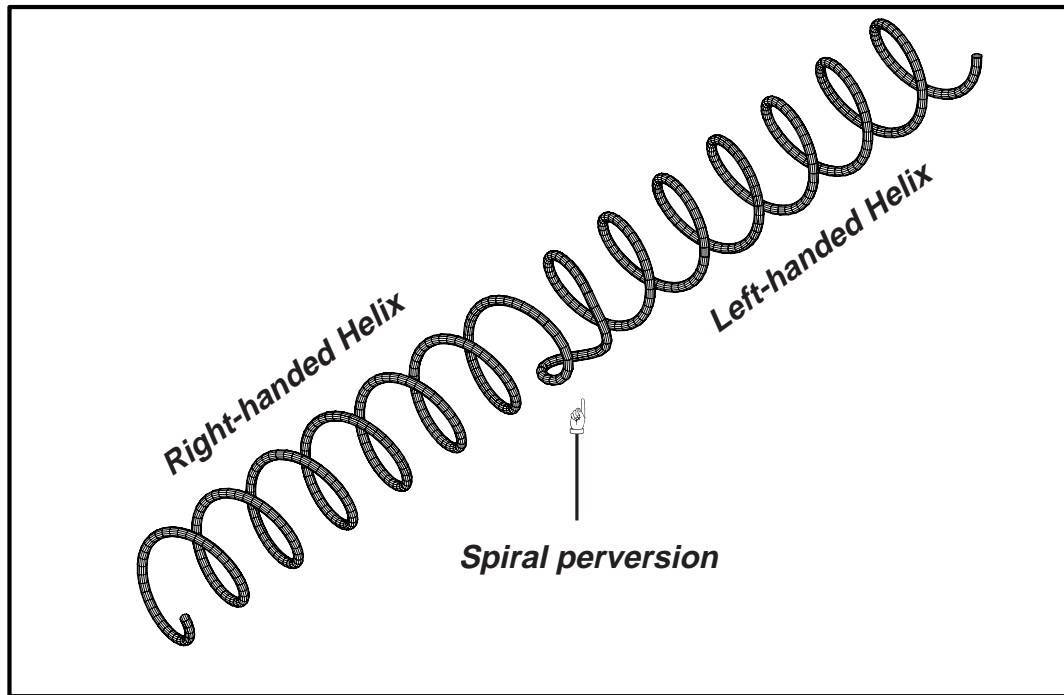


Figure 8: Helix-hand reversal for a straight filament, $K = 1/4$, $\Gamma = 1/4$, $n = 1/8$